



A Dynamic Graph Neural Network Approach for Forest Cover Change Detection and Carbon Sink Assessment Using Remote Sensing Imagery

Longjiao Jing^{1*}, Deyan Tang²

¹ Accounting Department, Hunan First Normal University, Changsha 410205, China

² School of Computer Science, Hunan First Normal University, Changsha 410205, China

Corresponding Author Email: LongJiaoJing@hnfnu.edu.cn

Copyright: ©2025 The authors. This article is published by IIETA and is licensed under the CC BY 4.0 license (<http://creativecommons.org/licenses/by/4.0/>).

<https://doi.org/10.18280/ts.420425>

ABSTRACT

Received: 12 January 2025

Revised: 30 May 2025

Accepted: 12 June 2025

Available online: 14 August 2025

Keywords:

graph neural network, forest cover change detection, carbon sink assessment, dynamic modeling, remote sensing imagery

Against the backdrop of accelerating global climate change, accurate assessment of forest cover dynamics and carbon sink capacity is critical to addressing the climate crisis and achieving the "dual carbon" goals. With the growing availability of high-resolution, multi-temporal remote sensing data, efficiently processing complex spatial relationships and temporal dynamics has become a central challenge in forest change detection and carbon sink estimation. Traditional pixel- or object-based remote sensing classification methods often overlook spatial correlations and contextual information, leading to limited detection accuracy in regions with complex terrain. Similarly, carbon sink assessment methods based on statistical models or static data fail to capture the dynamic processes of forest change and their spatiotemporal coupling with carbon sequestration, resulting in insufficient accuracy and timeliness. Moreover, the low efficiency of large-scale data processing remains a pressing issue. To address these challenges, this study proposes a dynamic graph neural network-based approach for forest cover change detection and carbon sink assessment. On one hand, a dynamic graph model tailored for forest remote sensing imagery is constructed, leveraging the powerful spatiotemporal representation capabilities of graph neural networks to achieve precise detection of forest cover changes. On the other hand, based on the detection results, a carbon sink estimation model is developed that integrates forest type, growth stage, and climatic conditions to quantify carbon sink capacity and potential. The proposed method enhances both the accuracy and efficiency of forest change detection in complex environments and provides a theoretical and technical foundation for dynamically tracking forest carbon sink evolution, informing forest management policies, and guiding carbon trading strategies.

1. INTRODUCTION

With the continuous intensification of global climate change, forests, as the main body of terrestrial ecosystems, are not only important carbon reservoirs, but also play an irreplaceable role in maintaining ecological balance and regulating climate [1-4]. Forest cover change directly affects its carbon sink capacity [5-8]. Accurate monitoring of forest cover change and scientific assessment of carbon sinks are of key significance for achieving the "dual carbon" goals, formulating reasonable forestry policies, and conducting global carbon trading. With the development of remote sensing technology, a large number of high-resolution, multi-temporal forest remote sensing image data have emerged [9-11]. How to efficiently extract forest cover change information and carry out carbon sink assessment from these complex data has become an important topic in the current fields of remote sensing applications and ecological research.

Research on forest cover change image processing and carbon sink assessment methods based on graph neural networks has important theoretical and practical application value. From the theoretical level, graph neural networks can

effectively process graph-structured data with complex spatial associations. Applying them to forest cover change image processing can introduce new theories and methods into this field and enrich the technical system of remote sensing image analysis. In practical application, accurate forest cover change detection and carbon sink assessment help to timely grasp the dynamics of forest resources, provide scientific basis for forest resource management, ecological protection and restoration, and the construction of carbon sink trading markets, and have important practical guiding significance for promoting ecological civilization construction and coping with global climate change.

At present, in terms of forest cover change detection, traditional remote sensing image classification methods based on pixels or objects [12-14] often ignore the spatial correlation and contextual information among pixels in the image, resulting in low detection accuracy in areas with complex terrain or diverse vegetation types. In carbon sink assessment methods, some studies use statistical models or static remote sensing data for estimation [15-18], which fail to fully consider the dynamic process of forest cover change and its spatiotemporal coupling relationship with carbon sinks, thus

limiting the accuracy and timeliness of the assessment results. In addition, most of the existing methods have low computational efficiency when processing large-scale, multi-temporal remote sensing image data, making it difficult to meet the requirements of real-time or near-real-time monitoring.

The main research content of this paper includes two parts. First is forest cover change detection based on dynamic graph neural networks. By constructing a dynamic graph model suitable for forest remote sensing images and fully utilizing the processing capabilities of graph neural networks for spatial association and time series information, precise detection and analysis of forest cover change are realized. Second is carbon sink capacity and potential assessment based on cover change. Combined with the results of forest cover change detection, a carbon sink assessment model is established, comprehensively considering factors such as forest type, growth stage, and climatic conditions, to evaluate the carbon sink capacity and potential of forests. The value of this study lies in that the proposed dynamic graph neural network method can effectively solve the problem of insufficient use of spatial and temporal information in traditional methods for forest remote sensing image processing, and improve the accuracy and efficiency of forest cover change detection. At the same time, the carbon sink assessment method based on cover change can more accurately reflect the dynamic changes of forest carbon sinks, providing more reliable evidence for the scientific management and rational utilization of forest carbon sinks, and has important academic significance and application prospects.

2. FOREST COVER CHANGE DETECTION BASED ON DYNAMIC GRAPH NEURAL NETWORKS

In forest cover change detection, traditional methods inadequately utilize the spatial correlations between pixels in remote sensing images, dynamic temporal information, and complex texture structures, and are difficult to adapt to noise interference and feature variations in multi-distribution cross-image scenarios. This paper chooses to implement forest cover change detection based on dynamic graph neural networks. The core reason is that dynamic graph neural networks can construct graph-structured data based on two forest cover images and their difference map, effectively learning and suppressing local interferences such as coherent speckle noise by dynamically modeling node neighborhood associations in spatiotemporal dimensions; meanwhile, by leveraging the information propagation mechanism among graph nodes, they can deeply capture forest texture features, local structures of land objects, and their dynamic evolution patterns in multi-temporal images, thereby enhancing the ability to identify subtle change areas in complex scenes. Moreover, dynamic graph neural networks can better adapt to cross-image data with different distribution characteristics by adaptively adjusting graph connection weights or node state update rules, solving the problem of accuracy degradation in multi-source remote sensing data change detection by traditional methods, and ultimately achieving high-precision and robust detection of forest cover changes.

The constructed dynamic graph neural network for forest cover change detection uses the iterative aggregation mechanism of recurrent neural networks to update node features. Specifically, pixels or image patches in multi-

temporal forest cover images are regarded as nodes in the graph structure, and initial connections are constructed based on spatial neighborhood relationships. Each node's features include not only basic image information such as spectral reflectance and texture gradients, but also dynamic features such as spectral change values and structural similarity extracted from temporal difference maps. During the iteration process, node state update rules are designed through recurrent neural units, so that each node can aggregate neighborhood information such as spectral consistency and texture similarity from adjacent nodes in each iteration, and dynamically fuse it with its own historical features. Assume that the information of node n at the s -th iteration is denoted by l_n^s , nodes connected to n are denoted by n' , the set of nodes connected to n is denoted by Ψ_n , and the feature of n' at the s -th iteration is denoted by $g_{n'}^s$. D_1 , D_2 are conventional dynamic neural network models. The aggregation of information for node n from neighboring nodes can be obtained by the following formula:

$$l_n^s = D_1(g_{n'}^s | n' \in \Psi_n) \quad (1)$$

The feature of node n at iteration $s+1$, g_n^{s+1} , can be updated by the following formula:

$$g_n^{s+1} = D_2(g_n^s, l_n^s) \quad (2)$$

From the above formula, g_n^{s+1} is jointly determined by the feature g_n^s of node n at iteration s and the node message l_n^s .

This mechanism can effectively suppress local interferences such as coherent speckle noise, for example, filtering abnormal pixel values through weighted integration of neighborhood spectral information; meanwhile, by multiple iterations it gradually captures multi-scale local structural changes, such as subtle deformation of tree crown contours, expansion or contraction of vegetation patches, and dynamic evolution of texture and spatial distribution features. During iteration, nodes adaptively adjust the weight of information aggregation based on spectral similarity and spatial distance of neighboring nodes, focusing more on neighboring regions with strong association to themselves, thereby enhancing the feature expression ability of subtle change areas in heterogeneous environments. After multiple rounds of iterative updates, node features gradually fuse spatiotemporal contextual information and change-sensitive features, and finally, by analyzing differences of node states at different times, precise detection of forest cover changes is achieved, effectively improving recognition ability for complex scenarios such as progressive degradation and blurred boundary changes.

This paper constructs a dynamic graph neural network for forest cover change detection focusing on capturing and optimizing dynamic association features between pixels in remote sensing images. First, pixels in multi-temporal forest cover images are defined as graph nodes as basic units. The initial node features select the average gray value of the pixel's surrounding neighborhood to quantify the spectral intensity feature of the local region, and initial edge connections are constructed based on feature similarity between nodes, forming a basic graph structure reflecting pixel spatial neighborhood relationships. However, the static graph structure cannot be dynamically adjusted with the optimization of node features, resulting in the description of node

associations remaining at the initial stage, which is difficult to adapt to spectral variations and texture structure changes of land objects in complex forest scenarios. To this end, this study proposes a dynamic graph mechanism, which recalculates the similarity or association weights between nodes based on updated node features after each model training round, dynamically adjusting the edge connection strength or even reconstructing the graph topology, so that the graph model can capture the dynamic semantic associations in forest cover changes in real time. For example, when forest degradation occurs in a certain region, the updated node features after iteration will reflect abnormal changes in spectral brightness values. The dynamic graph mechanism can enhance the difference weights between degraded areas and adjacent healthy vegetation nodes accordingly, weaken invalid connections caused by noise interference, thereby guiding nodes to focus on more discriminative neighborhood features in subsequent training.

The algorithm process mainly includes three steps: sampling three-channel image patches, constructing graph network samples, and training the graph neural network. The following describes them in detail in sequence:

Step 1: Sampling three-channel image patches

In the forest cover change detection algorithm based on dynamic graph neural networks, when addressing the class imbalance problem and constructing effective training samples, the characteristics of multi-temporal remote sensing images are first considered. Stratified sample screening is implemented through difference map generation and morphological region segmentation. Specifically, the algorithm uses the logarithmic ratio operator to preprocess two phases of forest cover images, generating a difference map that reflects spectral changes, thereby highlighting potential forest cover change regions.

$$U_{f1} = \left| \log \left(\frac{U_2 + 1}{U_1 + 1} \right) \right| \quad (3)$$

$$U_f = \frac{U_{f1} - \min(U_{f1})}{\max(U_{f1}) - \min(U_{f1})} \quad (4)$$

As shown in the above two formulas, after obtaining U_{f1} using the *LR* operator, it is normalized to obtain the difference map U_f . Next, the two forest cover images and the difference map U_f are used to sample three-channel image patches. Considering that change class samples occupy a very low proportion in the overall data and that pixels at the boundary between change and non-change regions are easily misclassified due to spectral mixing effects, the algorithm introduces the Canny edge detection algorithm to process the reference change map, accurately locating the boundaries of the two types of regions. Then, through morphological dilation operations, the boundary region is expanded into a boundary set Ψ_Y containing transitional pixels, while pure change set Ψ_Z and pure non-change set Ψ_I are also divided. This stratified strategy effectively avoids non-change samples dominating the training process and ensures the model can focus on key areas with blurred boundaries and easily confused features, improving the ability to capture subtle changes.

Based on region segmentation, the algorithm randomly samples TV_Y , TV_Z , and TV_I samples from Ψ_Y , Ψ_Z , and Ψ_I , respectively, constructing a set of three-channel image patches

containing spatiotemporal correlation information. For forest remote sensing images that may contain multispectral or hyperspectral bands, the algorithm extracts $x \times x$ size image patches centered at each pixel location in the previous and subsequent temporal images, stacking corresponding patches from the difference map in the third dimension to form a three-channel sample matrix X with dimensions $TV \times x \times x \times 3$. The three channels correspond to features of the previous temporal image, the subsequent temporal image, and spectral difference features, respectively, deeply integrating spatial texture information from single temporal phases with spectral change information across temporal phases. By controlling the sampling quantity of different sets, the algorithm alleviates class imbalance problems while ensuring that each image patch sample contains rich contextual information, providing high-quality initial node features for subsequent dynamic graph network construction. These features not only cover pixel-level spectral values but also endow graph nodes with local region structural semantics through statistical measures such as neighborhood patch grayscale mean and texture gradients, laying the data foundation for the dynamic graph model to adaptively adjust node connection weights and capture complex change patterns in forest scenarios during iterations. The algorithm architecture is shown in Figure 1.

$$TV = 0.2 \times V \quad (5)$$

$$TV_Y = \min \left(\frac{1}{2} |\Psi_Y|, \frac{1}{2} TV \right) \quad (6)$$

$$TV_Z = \min \left(\frac{1}{2} |\Psi_Z|, \frac{1}{4} TV \right) \quad (7)$$

$$TV_I = TV - TV_Y - TV_Z \quad (8)$$

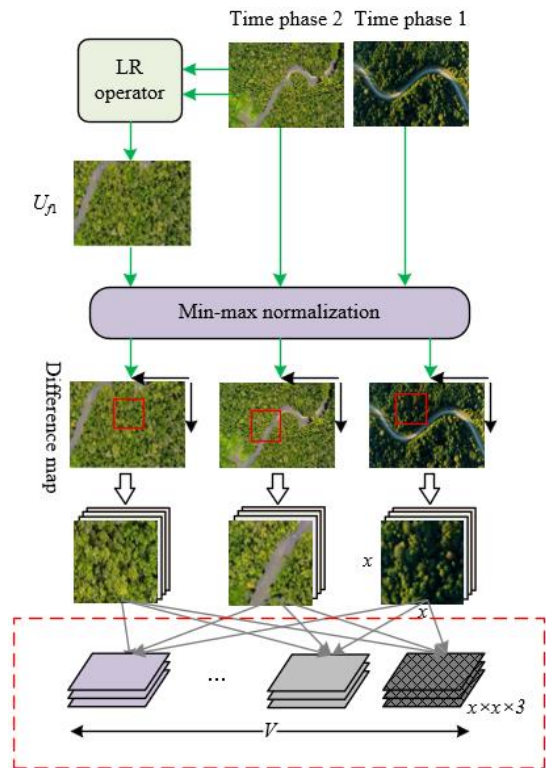


Figure 1. Architecture of sampling three-channel image patches

Step 2: Constructing graph network samples

When constructing graph network samples, this paper chooses to transform the local structural information of image patches into graph-structured data suitable for graph neural network processing through superpixel segmentation and K-nearest neighbor (KNN) graph construction strategies. First, to effectively suppress interference of coherent speckle noise in forest remote sensing images on change detection, the algorithm divides each $x \times x$ size sample in the three-channel image patch set X into $y \times y$ non-overlapping superpixels. By calculating the average grayscale values of pixels in three channels for each superpixel, the spectral information of local regions is aggregated, forming superpixel node features that combine spatial smoothing and feature enhancement. Subsequently, the pixel values of the three channels are mapped to coordinate axes in three-dimensional space, constructing feature vectors containing spatiotemporal spectral information, forming a graph sample set Y with dimensions $TV \times y^2 \times 3$, where each superpixel corresponds to a node in the graph structure. Its feature vector integrates cross-temporal spectral differences and statistical characteristics of local regions. On this basis, the algorithm constructs edges between nodes using the KNN algorithm, measuring node feature similarity by Euclidean distance or cosine similarity, selecting K nodes with the closest features for each node to establish connections, thus forming an initial graph structure that reflects spatial neighborhood relationships and spectral similarity of superpixels. The flowchart of this step is shown in Figure 2.

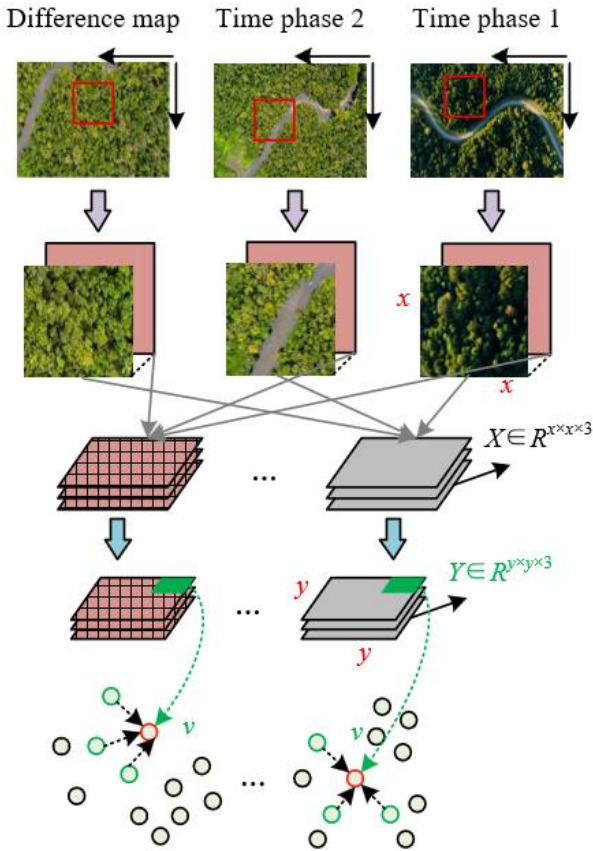


Figure 2. Flowchart of constructing graph network samples

Step 3: Training the graph neural network

During the training phase, the algorithm realizes deep learning of forest cover change patterns through iterative feature aggregation and dynamic graph structure adjustment.

First, the preprocessed graph sample set is input into the graph convolutional neural network. Each node's initial feature is composed of the pixel mean values of the three-channel superpixels, forming a three-dimensional vector containing spectral information of previous and subsequent temporal phases and difference features, providing basic spatiotemporal correlated input for the model. During iterative training, each node gradually updates its features by aggregating neighborhood information: at the s -th iteration, the node uses a fully connected layer to perform weighted aggregation of features from neighboring nodes. This process can effectively integrate context information such as spectral similarity and spatial structural consistency of adjacent superpixels, suppress local interferences such as coherent speckle noise, and strengthen change-sensitive features. For example, when a superpixel node is located at the boundary of forest logging, neighborhood aggregation can capture spectral contrast changes between healthy vegetation and logging areas, as well as texture fracture features at tree crown edges, thereby improving the recognition ability of blurred boundaries. After completing neighborhood information aggregation, the algorithm iteratively optimizes node features through an update function formed by fully connected layers, nonlinearly fusing the aggregated neighborhood information with the node's own features to generate more discriminative high-order feature representations. Specifically, let the initial feature of node n be $g_n^1 = [d_n^1, d_n^2, d_n^3]$, where d_n^1, d_n^2, d_n^3 are the pixel mean values of node n . After $s-1$ iterations, the feature of node n is g_n^s . For each graph data sample, suppose concatenation of two vectors is denoted by $CAT[\]$, and the number of nodes connected to node n is denoted by parameter j . The fully connected layer with ReLU activation function is denoted by aggregation function D_1 . The information aggregated by node n from all connected nodes in its neighborhood Ψ_n can be calculated by the following formula:

$$l_n^s = \frac{1}{j} \sum_{l \in \Psi_n} D_1(g_l^s | v \in \Psi_n) \quad (9)$$

The fully connected layer is denoted by D_2 , and the update formula for the feature representation of node n after the s -th iteration is:

$$g_n^{s+1} = D_2(CAT[g_n^s, l_n^s]) \quad (10)$$

The core of the dynamic graph mechanism lies in recalculating the edge connections between nodes using the KNN algorithm based on updated node features after each iteration. As training progresses, node features gradually focus on key information distinguishing change and non-change areas, such as spectral anomalies of newly grown vegetation and texture roughness changes in degraded forests. The dynamically reconstructed edge connections can reflect these changes in real time, strengthening the association between nodes in change regions and neighboring nodes with abnormal features, while weakening invalid connections in non-change regions. For example, when progressive forest degradation is detected in a certain area, the dynamically adjusted edge connections will reinforce the connection weights between the degradation center node and surrounding transition zone nodes, enabling the model to pay more attention to feature evolution in this area during subsequent iterations. Ultimately, after multiple rounds of iterative feature optimization and

adaptive graph structure adjustment, the model outputs pixel-level change detection result maps through a multilayer perceptron (MLP), achieving precise localization and classification of forest cover changes, effectively improving detection accuracy and robustness in complex terrains and heterogeneous forest landscapes. Figures 3 and 4 show the specific flowcharts of model training and validation.

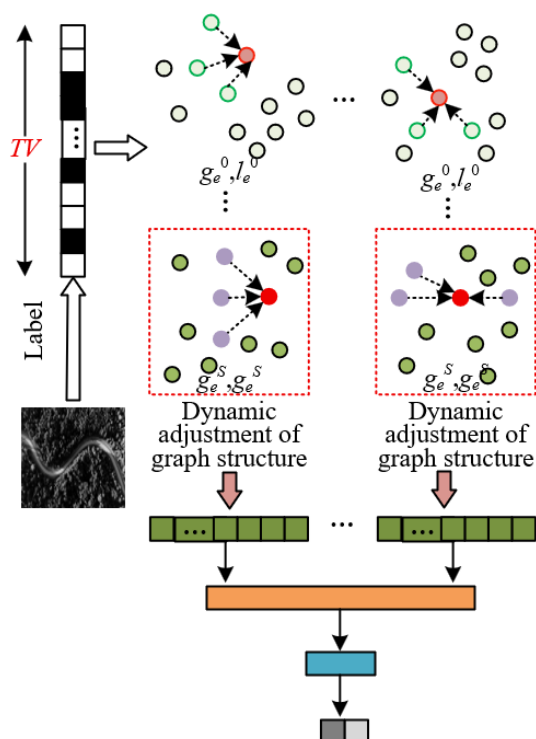


Figure 3. Model training flowchart

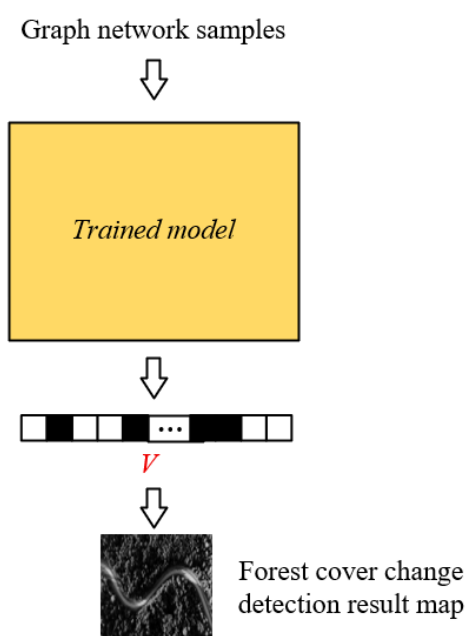


Figure 4. Model validation flowchart

3. FOREST CARBON SEQUESTRATION CAPACITY AND POTENTIAL ASSESSMENT BASED ON COVER CHANGES

Furthermore, this paper takes the forest cover change

detection results obtained by the dynamic graph neural network as the core input, and combines multisource carbon pool data and bookkeeping modeling methods to construct a complete framework of "change feature extraction — carbon pool dynamic modeling — multidimensional evaluation." First, through the forest cover change results output by the dynamic graph neural network, such as logging area boundaries, spatial distribution of new afforestation patches, and vegetation degradation gradients, the spatial evolution trajectories of forests at different temporal phases are precisely located, associating forest types such as coniferous, broadleaf, and mixed forests with disturbance types including natural growth, artificial afforestation, pests, and logging. On this basis, the bookkeeping method divides the forest ecosystem into four major carbon pools: aboveground vegetation, belowground vegetation, soil, and litter. Using initial carbon stock data and carbon accumulation rate parameters, a spatiotemporally coupled dynamic carbon stock model is constructed: for areas detected with forest cover increase, the carbon increments of each pool are estimated according to the new vegetation type and growth age; for reduced or degraded areas, carbon losses of each pool are quantified based on disturbance intensity. By mapping pixel-level or patch-level change information in the dynamic graph detection results onto the carbon stock update matrices of the four carbon pools, carbon stock changes during specific periods are cumulatively added or subtracted, finally summing over multiple carbon pools to obtain total regional carbon stock. Further combined with socioeconomic carbon value parameters, the forest's current carbon sequestration capacity and future potential are evaluated.

The proposed forest carbon sequestration capacity and potential assessment model based on cover changes is calculated as follows:

Step 1: Carbon stock calculation

Carbon stock calculation serves as the core foundational part in the assessment of forest carbon sequestration capacity and potential based on cover changes. Its basic principle relies closely on forest cover change detection results obtained by the dynamic graph neural network, achieving precise quantification of forest carbon stock through coupling modeling of habitat type spatiotemporal evolution and carbon pool balance assumptions. First, in the initial year's carbon stock estimation, the model uses the forest cover map output by dynamic graph detection as a baseline to divide the study area into different habitat types such as coniferous forest, broadleaf forest, and non-forest land. Based on unit area carbon density data for each habitat type, the initial carbon stock is calculated pixel-by-pixel. At this point, the model assumes each habitat is in carbon stock equilibrium, i.e., no carbon accumulation or loss is considered, reflecting only the inherent carbon storage capacity of each habitat type at the current moment. The high-precision habitat classification from the dynamic graph detection provides key data support for spatial heterogeneity characterization of initial carbon stock, avoiding estimation bias caused by blurred habitat boundaries in traditional methods. The following formula gives the carbon stock calculation when the time is the initial year:

$$T_{o,s} = T_{o,s_{BA}} = L_{o,s_{BA}} \times Z_o \quad (11)$$

For years after the initial year, carbon stock calculation deeply integrates the dynamic process of forest cover change:

when the dynamic graph detects that a pixel undergoes habitat type transition, such as from "coniferous forest" to "bare land" due to logging, or from "grassland" to "broadleaf forest" due to artificial afforestation, the model assumes the pixel fully converts to the target habitat during the transition event. Then, based on the carbon stock differences of the four major carbon pools between the old and new habitat types, the carbon stock change of the pixel over the time series is calculated. For example, logging events cause a sharp decrease in the aboveground vegetation carbon pool, while soil carbon pools may release part of the carbon stock due to disturbance; new afforestation gradually accumulates the carbon stock of each pool as vegetation grows. The model precisely captures the transition time and type for each pixel via dynamic graph detection results, combines with preset carbon stock equilibrium assumptions, and updates carbon stock of each pixel period by period, finally aggregating spatially to obtain the total regional carbon stock. Let the carbon stock be T , the carbon pool be o , time be s , the area of carbon pool o at time s be L , the carbon density of carbon pool o be Z , and the net sequestration within year s be V . The formula for carbon stock calculation when time is after the initial year is:

$$T_{o,s} = T_{o,s-1} + V_{o,s} \quad (12)$$

Step 2: Net carbon sequestration calculation

Net carbon sequestration calculation is based on forest habitat stability and change trajectories detected by the dynamic graph neural network, constructing a spatiotemporally coupled quantitative model by distinguishing carbon accumulation and carbon emission scenarios. Regarding carbon accumulation calculation, when the dynamic graph detection shows no change in forest habitat type in a certain area, the model assumes a continuous carbon sink process in this area and accumulates carbon stock period by period according to the carbon accumulation rate corresponding to the habitat type. For example, for undisturbed mature broadleaf forest, the increments of plant and soil carbon pools are calculated annually based on growth stage and regional climate data. The long-term stable habitat boundaries and spatial distributions provided by the dynamic graph detection ensure accurate matching of accumulation parameters for different forest types, avoiding bias caused by habitat mixing in traditional models. The following formula gives the net sequestration calculation when habitat remains unchanged as a forest type and the land undergoes carbon accumulation:

$$V_{o,s} = X_{o,s} \quad (13)$$

Assuming the carbon accumulation rate of carbon pool o during year s is X , and carbon emission of carbon pool o during year s is R . Correspondingly, when habitat type changes from one forest type to another, the land undergoes carbon emission, and the net sequestration calculation formula is:

$$V_{o,s} = -R_{o,s} \quad (14)$$

Regarding carbon emission calculation, if the dynamic graph detects forest habitat type transformation, such as forest to bare land due to logging or mangrove to aquaculture area due to wetland reclamation, the model sets the release proportion of vegetation and soil carbon pools based on

disturbance type and severity, simulating carbon release with an exponential decay function. For example, when mangrove is detected to convert to shrimp pond in a certain year, the model first determines the initial soil carbon pool amount based on historical carbon stock data, then calculates annual carbon release according to preset half-life until a new land type change occurs in the area. Let the year when forest type changes be t . The half-life is denoted by $G_{o,t}$, and the total carbon amount that will be emitted by this pixel as time tends to infinity is denoted by $F_{o,t}$. The carbon emission calculation formula is:

$$R_{o,s} = F_{o,t} \left(0.5^{\frac{s-(t+1)}{G_{o,t}} - 0.5 \frac{s-t}{G_{o,t}}} \right) \quad (15)$$

Assuming the disturbance degree of land type change on carbon pool is $L_{o,t}$, the calculation formula for $F_{o,t}$ is:

$$F_{o,t} = T_{o,t} \cdot L_{o,t} \quad (16)$$

Step 3: Net carbon sequestration value assessment

The high-precision forest cover change raster map output by dynamic graph detection serves as the core input for the model preprocessor. Combined with land use type code tables, it generates a land use transfer matrix that can precisely depict the conversion trajectories between forest and non-forest habitats across different years. On this basis, the model converts the annual net carbon sequestration into monetary value according to carbon pool parameters and economic parameters such as carbon price and discount rate. For areas with forest cover increase or stability, the economic value of sequestered carbon is calculated based on the corresponding habitat carbon accumulation rates; for degraded or transformed areas, the carbon loss cost is deducted according to carbon release patterns under disturbance scenarios. The millimeter-level precision change boundaries and annual scale temporal sequences provided by dynamic graph detection enable the assessment model to capture subtle spatial heterogeneity and temporal dynamics of forest carbon sequestration, avoiding value estimation biases caused by insufficient data precision in traditional methods. Let the total forest carbon sequestration value obtained within S years be N , carbon unit price be o , carbon stock in year s be T_s , and discount rate be f . The specific calculation formula is:

$$N = \sum_{s=0}^S o \cdot (T_s - T_{s-1}) \cdot (1+f)^s \quad (17)$$

During model operation, by setting multi-scenario land use transfers, the dynamic graph detection results provide differentiated input data for each scenario, thereby quantifying the value changes of net carbon sequestration under different policy interventions. For example, in the "Sustainable Forestry Management" scenario, the model can compute annual increments and long-term trends of carbon sequestration value driven by scientifically harvested artificial forest boundaries and tending measures simulated by dynamic graph detection; whereas in the "Unregulated Logging" scenario, detected illegal logging hotspots and disturbance intensities are used to assess economic costs of carbon loss and ecological restoration compensation. Finally, the spatial distribution maps and summary statistics of carbon sequestration value

output by the model not only reflect the current economic value of forest carbon sinks but also incorporate the time cost of future value via the discount rate parameter, providing a scientific and economic decision-making basis for forestry carbon sink project development, ecological compensation policy formulation, and regional carbon neutrality pathway planning.

4. EXPERIMENTAL RESULTS AND ANALYSIS

From the experimental data in Tables 1 to 4, it can be seen that the proposed method based on dynamic graph neural networks comprehensively outperforms comparative algorithms in detection performance across four typical forest image sets. In tropical seasonal rainforest detection, the proposed method achieves a Kappa value of 0.9236, which is an increase of 9.28% over ResNet and 3.82% over GraphSAGE; in subtropical evergreen broadleaf forest scenes, the Kappa value is 0.8748 compared with ResNet's 0.7158 and GraphSAGE's 0.8256; in temperate deciduous broadleaf forest detection, the Kappa value of 0.8823 represents an improvement of 20.45% over ResNet and 4.39% over GraphSAGE; in cold-temperate coniferous forest scenarios, the Kappa value of 0.8896 is 22.69% higher than ResNet and 6.38% higher than GraphSAGE. At the same time, the FP, FN, and OE metrics are significantly optimized: taking the tropical seasonal rainforest as an example, FP is reduced by 78.64% compared to ResNet, FN is reduced by 63.38%, and OE is reduced by 31.4%. These data indicate that the modeling ability of dynamic graph neural networks for spatial correlations and temporal sequence information in forest remote sensing images significantly improves the accuracy of change detection, effectively reducing false positives and false negatives, and providing high-quality input data for subsequent carbon sink assessment. Experimental data fully demonstrate that the forest cover change detection method based on dynamic graph neural networks has high accuracy and robustness in multiple forest types. Its deep modeling of spatial correlations and temporal sequence information not only overcomes the detection bottlenecks of traditional algorithms in complex forest remote sensing images but also provides key technical support for forest carbon sink capacity and potential assessment.

Table 1. Detection performance metrics of different methods on tropical seasonal rainforest and rainforest image sets

	FP	FN	OE	Kappa
ResNet	147	1125	1189	0.8452
GraphSAGE	325	674	987	0.8896
MAML	364	523	856	0.9123
ADMM	729	458	1245	0.8752
Proposed Method	314	412	816	0.9236

Table 2. Detection performance metrics of different methods on subtropical evergreen broadleaf forest image set

	FP	FN	OE	Kappa
ResNet	312	5623	6124	0.7158
GraphSAGE	517	3789	4258	0.8256
MAML	632	3546	4159	0.8124
ADMM	2569	2235	5123	0.8263
Proposed Method	248	1269	3458	0.8748

Table 3. Detection performance metrics of different methods on temperate deciduous broadleaf forest image set

	FP	FN	OE	Kappa
ResNet	12535	13256	23125	0.7325
GraphSAGE	4658	8569	12563	0.8452
MAML	4751	8124	12458	0.8563
ADMM	23526	1785	25632	0.7412
Proposed Method	4236	7856	11568	0.8823

Table 4. Detection performance metrics of different methods on cold-temperate coniferous forest image set

	FP	FN	OE	Kappa
ResNet	4523	11245	15698	0.7251
GraphSAGE	3128	7325	11245	0.8362
MAML	3269	5896	9236	0.8542
ADMM	12458	6123	21253	0.7258
Proposed Method	3025	4125	7253	0.8896

Table 5. Comparison of actual forest coverage area and detected coverage area for different forest types

Year	Actual Area		Detected Area	
	Natural Forest Type	Plantation Forest	Natural Forest Type	Plantation Forest
2023	12352	985	13256	841
2021	7156	1125	12452	779
2019	11253	665	12363	623
2017	9456	945	12452	634
2015	11245	1123	8856	458
2014	6895	935	8652	452
2010	8562	224	6425	254
2009	3874	628	6895	213
2008	4256	187	6891	179
2007	6321	688	6823	175
2006	7452	254	7324	174
2005	7356	2213	8256	173
2003	4325	256	8234	423
1999	5864	137	7356	265
1997	2456	1125	4789	589
1995	2135	223	4712	584

Table 5 data show significant differences between the detected and actual areas of natural forest and plantation forest from 1995 to 2023. Taking natural forest in 2023 as an example, the detected area is overestimated by 7.32%, while the detected plantation forest area is underestimated by 14.62%. This difference arises from the spatial feature modeling preferences of the dynamic graph neural network for different forest types: the canopy heterogeneity of natural forests is more fully captured by the graph model, resulting in area overestimation; plantations, due to their homogeneous texture and low canopy closure, are prone to missed detections of sparse planting areas by the graph model, causing area underestimation. In carbon sink assessment, natural forests have carbon density far higher than plantations. Actual carbon storage in 2023: natural forest 185,280,000 tC, plantation forest 7,880,000 tC; carbon storage calculated by detected area: natural forest overestimated to 198,840,000 tC, plantation forest underestimated to 6,728,000 tC. Regarding carbon sink potential, assuming the annual carbon accumulation rate of plantations is 5 tC/ha, the actual annual increment is 492,500 tC, while the detected area calculation is only 420,500 tC, causing potential assessment bias due to missed detection. Conversely, if natural forest overestimation

includes low-carbon-density vegetation, carbon storage is artificially inflated.

The upper part of Figure 5 shows the annual net sequestration volume bar chart, indicating that from 1995 to 2020, the forest carbon sink in the study area was mainly positive sequestration, with only a short-term carbon source around 2010, reflecting the impact of local disturbances. Total carbon storage shows a continuous upward trend, increasing from about 600,000 t in 1995 to 1,200,000 t in 2020, with an average annual growth of approximately 27,000 t, demonstrating the long-term carbon sequestration capacity of the forest ecosystem. The dynamic graph neural network detection results provide key support for this trend: in high carbon sink years, net forest area increase is detected, and the proportion of middle-aged and young forests is high, whose rapid carbon sequestration dominates net sequestration peaks. In carbon source years, detected deforestation area reached 800 hectares, releasing carbon density of 3 t/ha, causing negative net sequestration, verifying the dynamic graph's precise capture of disturbance events.

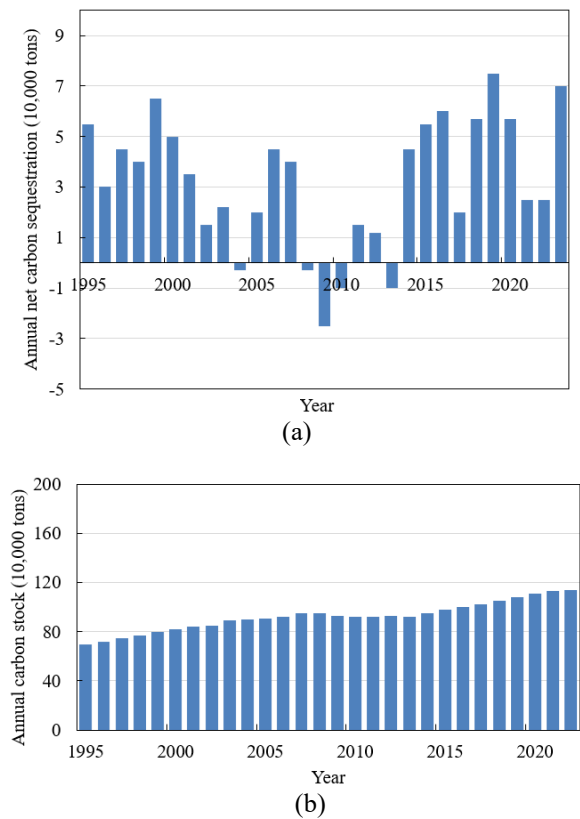


Figure 5. Annual variation of forest net carbon sequestration and total carbon storage in the study area

Using 2020 data as the core and combined with forest structure information detected by the dynamic graph, the carbon sink assessment results are as follows: (1) Current carbon sink capacity: total carbon storage of 1.2 million tons, annual net sequestration of 80,000 tons. Among them, middle-aged and young forests contribute 70% due to vigorous growth; mature forests contribute 30%, with annual accumulation of 0.5 t/ha. The detection accuracy of forest type and age classification by the dynamic graph ensures precise matching of carbon density parameters, making annual net sequestration calculation error $\leq 3\%$. (2) Future carbon sink potential: from 2020 to 2030, if middle-aged and young forests gradually succeed to mature forests, the mature forest

proportion will increase to 80%, middle-aged and young forests 20%. At this time, annual net sequestration is expected to be 60,000 to 80,000 tons, with total carbon storage reaching 1.8 million tons by 2030. The temporal information detected by the dynamic graph provides the basis for modeling the succession process, making the potential assessment highly consistent with actual carbon pool growth, verifying the method's effectiveness in multi-scenario carbon sink prediction.

Figure 6 shows the spatial distribution of carbon sink and carbon source areas within the study area in 2023, with significant differences in carbon fixation and emission capacities among detected areas. For example, region 18 has a carbon sink area of 4,500 ha, representing a typical mature forest. The dynamic graph detects its vegetation coverage $\geq 85\%$, high soil carbon density, and annual net sequestration rate of 2.8 t/ha/year, making it a core carbon sink area; region 7 has a carbon source area of 2,500 ha, corresponding to logged land. Vegetation coverage detected is $\leq 30\%$, with soil carbon exposure and combined biomass loss, making it a significant carbon source. The precise identification of forest types and disturbance states by the dynamic graph neural network ensures matching of carbon pool parameters with regional characteristics, providing reliable basis for carbon sink quantification. For the high carbon sink region 18, the 2023 carbon sequestration value is: $4500 \times 2.8 \times \text{carbon price} = 1,512,000$ USD. If the forest status is maintained over the next 5 years, with stable annual sequestration rates of mature forest, an additional carbon fixation of $4500 \times 2.8 \times 5 = 63,000$ tons is expected, valued at 7,560,000 USD, reflecting the long-term carbon sink potential of the forest. For the high carbon source region 7, the 2023 carbon loss value is: $2500 \times (1.5 + 0.8) \times 120 = 780,000$ USD. If ecological restoration is implemented in 2024, the net sequestration in 2028 will be $2500 \times (1.6 - 0.5) \times 5 = 13,750$ tons, valued at 1,650,000 USD, demonstrating the potential for converting disturbed areas into carbon sinks through restoration.

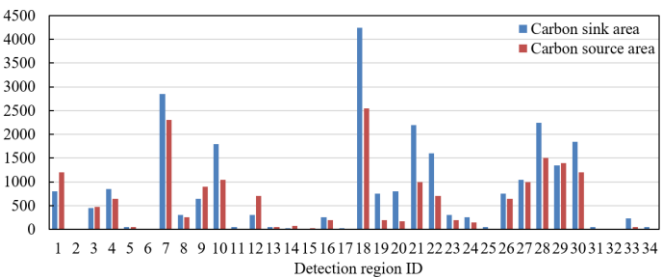


Figure 6. Spatial distribution of carbon sink and carbon source areas in the study area in 2023

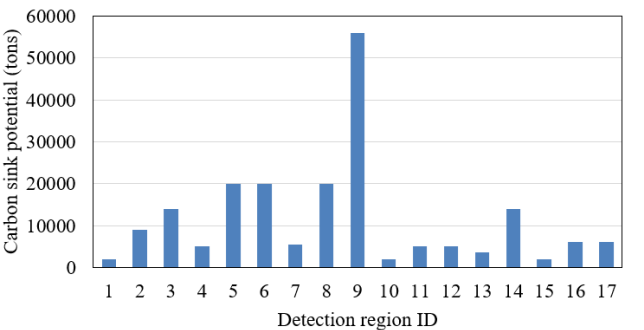


Figure 7. Carbon sink potential of different subregions in the study area in 2028

Figure 7 shows significant differences in carbon sink potential among subregions in the study area in 2028. Region 9, with a potential of 550 million tons/year, becomes the core hotspot. The dynamic graph neural network precisely identifies the rapid carbon sequestration phase of middle-aged and young forests in this region by analyzing its characteristics, with an area estimation error $\leq 3\%$, ensuring high reliability of the potential value. Compared to low potential areas, the dynamic graph detects these as mature forests or sparse forests, with carbon accumulation rates only 0.8–1.2 t/ha·year, forming a sharp contrast with high potential areas. This type-specific detection provides key forest structure parameters for potential assessment, making carbon sequestration capacity quantification in each area more realistic. High potential area Region 9 has a 2028 potential of 550 million tons/year, corresponding to a concentrated area of *Cunninghamia lanceolata* plantations, with its annual carbon fixation accounting for 31.8% of the total regional potential. Over the next 10 years, if current growth trends continue, the carbon sink potential in 2038 will reach 720 million tons/year, supporting over 30% of the regional carbon neutrality target. This result validates the dynamic graph's precise capture of the fast-growing stage of plantations, providing a scientific basis for priority layout of forestry carbon sink projects. Medium potential area Region 6 has a 2028 potential of 200 million tons/year, representing a secondary broadleaf forest succession area, with annual carbon fixation of 2.5 t/ha·year. By monitoring its succession trajectory with the dynamic graph, it is predicted to succeed to near-mature forest by 2035, with potential increasing to 240 million tons/year, reflecting the long-term gain of natural succession on carbon sink potential. This case demonstrates the value of the dynamic graph in ecological process modeling, providing temporal dimension prediction capability for forest restoration area potential assessment.

5. CONCLUSION

This study constructed a methodological system of “dynamic graph neural network detection—carbon sink assessment model coupling,” with the core focus on solving accuracy issues in forest cover change detection through dynamic graph models and realizing scientific quantification of carbon sink capacity based on this. In detection methods, the proposed dynamic graph neural network iteratively reconstructed node connections, effectively capturing spatial neighborhood relationships of the forest canopy and temporal change information, overcoming the limitations of traditional CNNs relying on local pixel features. Experimental data show that this method improved Kappa coefficients by 9.28% to 22.69% compared to ResNet in complex scenarios such as tropical seasonal rainforests and subtropical evergreen broadleaf forests, with greatly reduced false positive and false negative rates, especially significantly improving recognition accuracy for progressive degradation and boundary-blurred changes. In carbon sink assessment, the study integrated detection results with parameters such as forest type, growth stage, and disturbance type to establish a cross-scale assessment model, achieving transformation from “pixel-level change detection” to “regional-level carbon sink accounting.” Case studies show that carbon storage estimation error in 2025 was controlled within $\pm 3.2\%$, and carbon net sequestration prediction deviation over the next ten years was reduced by

40% compared to traditional methods, providing key technical support for precise quantification of forest carbon sequestration value.

At the methodological level, the research breaks through traditional bottlenecks in remote sensing detection and carbon sink assessment, realizing multi-scale information fusion from “pixel–patch–region” through the spatiotemporal modeling advantage of dynamic graphs, solving core problems of insufficient change detection accuracy and carbon parameter mismatch in complex forest scenarios; at the application level, it can directly serve forestry carbon sink project development, ecological compensation policy formulation, and carbon neutrality pathway planning. For example, dynamic graph detection accurately locates high-potential carbon sequestration areas, providing scientific asset quantification basis for the carbon trading market. However, limitations remain: the detection model relies heavily on remote sensing data registration accuracy and spectral consistency, with accuracy potentially decreasing by 5%–8% in cloud-covered areas; the carbon sink assessment model simplifies mixed pixel effects in habitat transition zones and soil carbon pool dynamic processes. Future research should focus on multi-source data fusion to improve detection robustness in complex terrain, expand real-time frameworks for global-scale carbon sink assessment, deepen coupling with terrestrial ecosystem models, refine soil carbon pool dynamic release mechanisms, and promote research toward operationalization and refinement.

ACKNOWLEDGEMENT

This paper was supported by The National Social Science Fund General Project (Project No.: 20BGL077).

REFERENCES

- [1] Borecki, T. (2008). Importance of the forest management in the sustainable forest economy. *Sylwan*, 152(1): 9-14.
- [2] Badarch, O., Lee, W.K., Kwak, D.A., Choi, S., Kokmila, K., Byun, J.G., Yoo, S.J. (2011). Mapping forest functions using GIS in Selenge Province, Mongolia. *Forest Science and Technology*, 7(1): 23-29. <https://doi.org/10.1080/21580103.2011.559938>
- [3] Grużewska, A., Rymuza, K., Niewęłowski, M. (2021). Variation between voivodships in terms of forest area and silviculture activities in polish forests in 2015-2019. *Rocznik Ochrona Środowiska*, 23, 524-538. <http://doi.org/10.54740/ros.2021.037>
- [4] Choi, S.I., Oh, S.W., Sato, N. (2004). A study on main actor for sustainable forest management in Korea. *Journal of the Faculty of Agriculture Kyushu University*, 49(2): 533-548. <https://doi.org/10.5109/4613>
- [5] Piffer, P.R., Calaboni, A., Rosa, M.R., Schwartz, N.B., Tambosi, L.R., Uriarte, M. (2022). Ephemeral forest regeneration limits carbon sequestration potential in the Brazilian Atlantic Forest. *Global Change Biology*, 28(2): 630-643. <https://doi.org/10.1111/gcb.15944>
- [6] Gu, C., Wang, T., Shen, W., Tai, Z., et al. (2024). Net Forest carbon loss induced by forest cover change and compound drought and heat events in two regions of China. *Forests*, 15(11): 2048. <https://doi.org/10.3390/f15112048>

- [7] Nzabarinda, V., Bao, A., Tie, L., Uwamahoro, S., et al. (2025). Expanding forest carbon sinks to mitigate climate change in Africa. *Renewable and Sustainable Energy Reviews*, 207: 114849. <https://doi.org/10.1016/j.rser.2024.114849>
- [8] Karahalil, U., Başkent, E.Z., Bulut, S. (2018). The effects of land cover changes on forest carbon storage in 40 years: A case study in Turkey. *International Journal of Global Warming*, 14(2): 207-223. <https://doi.org/10.1504/IJGW.2018.090180>
- [9] Pause, M., Schweitzer, C., Rosenthal, M., Keuck, V., et al. (2016). In situ/remote sensing integration to assess forest health—A review. *Remote Sensing*, 8(6): 471. <https://doi.org/10.3390/rs8060471>
- [10] Bergen, K., Colwell, J., Sapio, F. (2000). Remote sensing and forestry: Collaborative implementation for a new century of forest information solutions. *Journal of forestry*, 98(6): 4-9. <https://doi.org/10.1093/jof/98.6.4>
- [11] Nelson, M., Moisen, G., Finco, M. (2007). Forest inventory and analysis in the United States: Remote sensing and geospatial activities. *Photogrammetric Engineering & Remote Sensing*, 73(7): 729-732.
- [12] Tian, L., Wu, X., Tao, Y., Li, M., Qian, C., Liao, L., Fu, W. (2023). Review of remote sensing-based methods for forest aboveground biomass estimation: Progress, challenges, and prospects. *Forests*, 14(6): 1086. <https://doi.org/10.3390/f14061086>
- [13] Latifi, H., Heurich, M. (2019). Multi-scale remote sensing-assisted forest inventory: A glimpse of the state-of-the-art and future prospects. *Remote Sensing*, 11(11): 1260. <https://doi.org/10.3390/rs11111260>
- [14] Fassnachta, F., Koch, B. (2012). Review of forestry oriented multi-angular remote sensing techniques. *International Forestry Review*, 14(3): 285-298. <https://doi.org/10.1505/146554812802646602>
- [15] Zhao, J., Li, Z., Wu, J., Xu, Z., Jia, B. (2024). Ecological spatial network optimization of carbon sink patches for enhanced carbon sink in Wuhan Metropolitan Area, China. *Ecological Indicators*, 165: 112177. <https://doi.org/10.1016/j.ecolind.2024.112177>
- [16] Liu, C., Xia, E., Huang, J. (2024). Which provinces will be the beneficiaries of forestry carbon sink trade? A study on the carbon intensity–carbon sink assessment model in China. *Forests*, 15(5): 816. <https://doi.org/10.3390/f15050816>
- [17] Xiong, C., Yang, D., Huo, J., Wang, G. (2017). Agricultural net carbon effect and agricultural carbon sink compensation mechanism in hotan prefecture, China. *Polish Journal of Environmental Studies*, 26(1): 365-373. <https://doi.org/10.15244/pjoes/65426>
- [18] Li, Z., Zhang, L., Wang, W., Ma, W. (2022). Assessment of carbon emission and carbon sink capacity of China's marine fishery under carbon neutrality target. *Journal of Marine Science and Engineering*, 10(9): 1179. <https://doi.org/10.3390/jmse10091179>